

LT AND *Dst* DEPENDENCE OF THE RING CURRENT

A.A. Ostapenko and Yu.P. Maltsev (*Polar Geophysical Institute, Apatity*)

Abstract. Spatial distribution of the ring current flowing at $|z| < 3 R_E$ at five levels of *Dst*, five levels of the interplanetary magnetic field (IMF) z component, and five levels of the solar wind dynamic pressure P_{sw} has been found from magnetic data. The maximum of the current is located near midnight at distances of 6-8 R_E . The nightside part of the ring current at distances from 4 to 9 R_E grows with the storm activity, southward IMF, and solar wind pressure increasing. The dayside ring current is several times weaker and poorly correlates with either of the above geophysical parameters. The divergence of the ring current enables to calculate the region 2 field-aligned currents as well as the partial ring current (PRC), which intensity and dawn-to-dusk asymmetry are mostly controlled by P_{sw} . The PRC peak magnitude can be approximated as I_{PRC} (MA) = $0.26 + 0.55 P_{sw} - 0.15 B_z \text{IMF} - 0.023 Dst$, where $B_z \text{IMF}$ is the IMF southward component.

1. Introduction

The ring current flows in the stable trapping region at distances smaller than 10 R_E (R_E is the Earth radius). The ring current is commonly divided into the symmetric ring current and partial ring current. The partial ring current is closed to the region 2 field-aligned currents. The ring current is carried predominantly by protons with energy of 10-100 keV. During strong magnetic storms the ions of O^+ also contribute to the ring current [Daglis *et al.*, 1999].

There are a lot of case studies of energetic particles in the ring current region. Sometimes the ring current grows during storms [Frank, 1967; Smith and Hoffman, 1973; Lui *et al.*, 1987; Hamilton *et al.*, 1988; Spence *et al.*, 1989], sometimes it drops [Korth and Friedel, 1997; Kalegaev *et al.*, 1998; Dremukhina *et al.*, 1999]. Statistical studies are not numerous. Lui and Hamilton [1992] obtained plasma pressure radial profiles from $L = 2$ to $L = 9$ at noon and at midnight under quiet conditions. De Michelis *et al.* [1999] using AMPTE-CCE data have obtained energetic plasma profiles in four LT sectors for two AE ranges. The profiles appeared to be independent of both LT and AE. The ring current calculated from the magnetostatic equilibrium condition appeared to be several times stronger at midnight than at noon. Greenspan and Hamilton [2000] utilized the particle measurements for checking the Dessler-Parker-Sckopke (DPS) formula, which relates the total energy content of the trapped particles to the geomagnetic storm time depression *Dst*. In the nightside sector the energy content at distances of $2 < L < 7$ appeared to agree well with the DPS formula, whereas in the dayside there is no essential correlation between the *Dst* variation and energy content. Turner *et al.* [2001] when checking the DPS formula based on the *Polar* satellite data found that under a weak activity the trapped particles

provide ~75% contribution to *Dst*. Under *Dst* = -100 nT the contribution of the particles at the dayside drops down to 40%.

In this paper we study the ring current from magnetic data.

2. Data processing technique

The database of Fairfield *et al.* [1994] contains about 70,000 three-component magnetic field measurements obtained from 11 satellites at distances from 3 to 60 R_E for 20 years. All data are provided with the *Dst* values. For about 60% of the data hourly solar wind parameters are available. The data in the disk of $(x^2 + y^2)^{1/2} < 10 R_E$, $|z| < 4 R_E$ were utilized, where the coordinates are in the SM system. We divided the whole data-set into five subsets for five ranges of *Dst*, then for five ranges of $B_z \text{IMF}$, and five ranges of solar wind dynamic pressure $P_{sw} = m n V^2$ where m , n , and V are the proton mass, number density, and velocity, respectively.

For each subset the electric current surface density inside the layer of the width $\pm 3 R_E$ near the equatorial plane was calculated from the following formula

$$\mathbf{J}_\perp = \int_{-z_0}^{z_0} \mathbf{j}_\perp dz = \frac{1}{\mu_0} \oint [\mathbf{B} \times d\mathbf{l}] \quad (1)$$

As an integration contour we adopt a rectangle with the vertical side of $-z_0 < z < z_0$ where $z_0 = 3 R_E$ and horizontal size of 1 R_E . The external magnetic field was running averaged in bins with the horizontal sizes of 3 R_E . The vertical scale of averaging was 2 $R_E < |z| < 4 R_E$ for the horizontal magnetic components (B_x and B_y) and $-3 R_E < z < 3 R_E$ for the vertical magnetic component B_z . In order to increase the accuracy we assumed the north-south symmetry.

3. Azimuthal currents in the magnetosphere

Distribution of the azimuthal current for five ranges of *Dst*, five ranges of $B_z \text{IMF}$, and five ranges of P_{sw} is shown in Figure 1. One can see that the currents grow with enhancement of storm time activity, southward IMF, and solar wind dynamic pressure. Strong day-night asymmetry is evident, the nightside current density being several times greater than the dayside one. The current is maximum at $L \approx 6 - 8$. There is no pronounced dependence of the maximum on LT or geomagnetic activity.

Figure 2 shows the total current flowing at radial distances from 4 to 9 R_E in four local time sectors. One can see the growth of the ring current with the *Dst*, southward IMF, and P_{sw} in the nightside. In the dayside the ring current is several times weaker and does not reveal any pronounced dependence on *Dst*, $B_z \text{IMF}$, and P_{sw} .

The calculated radial component of the magnetospheric current is weaker than the azimuthal one by

about an order of magnitude, so it is not shown here.

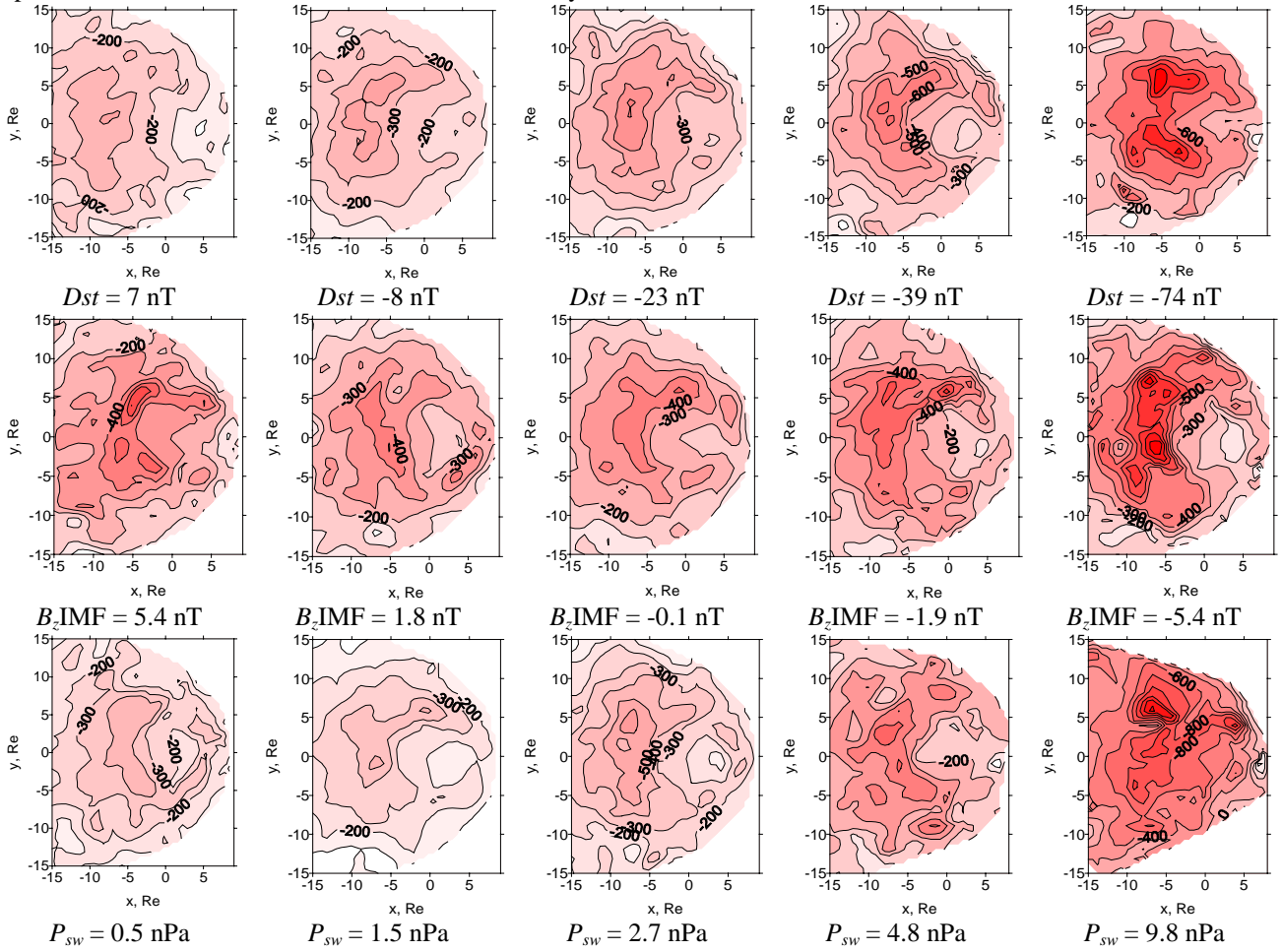


Figure 1. Surface density (in kA/R_E) of the eastward component of the electric current in the sheet of $-3 < z < 3R_E$.

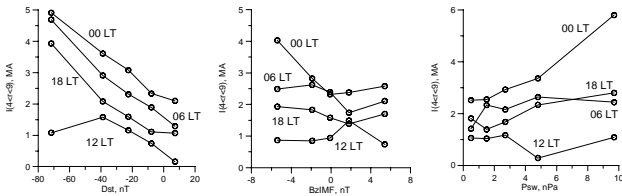


Figure 2. Total current flowing at radial distances from 4 to 9 R_E versus (left) Dst , (middle) $B_z IMF$, and (right) P_{sw} in four LT sectors.

4. Region 2 field-aligned currents and partial ring current

As it is seen from Figure 1, the magnetospheric current is evidently divergent, i.e. partly closed to the field-aligned currents (FACs). The FAC density can be calculated as follows

$$j_z(z=3) = -\frac{1}{2} \text{div} \mathbf{J}_\perp = -\frac{1}{2} \left(\frac{\partial J_x}{\partial x} + \frac{\partial J_y}{\partial y} \right) \quad (2)$$

Unfortunately, direct calculation of j_z from experimental J_x and J_y is hardly possible because of a large scattering of the data. So we preliminarily approxi-

mated J_x and J_y by polynomials of the fourth order of x and y in the distance range from 4 to 10 R_E . The relative residual error of the fitting varied from 2% to 24% in different subsets. Then the FACs were calculated using expression (2). Figure 3 shows the distribution of j_z . One can see that the FACs flow out of the magnetospheric current sheet in the dusk and flow into the sheet in the dawn. At the ionosphere level the FACs flow, correspondingly, into the ionosphere at the dusk and out of the ionosphere at the dawn, i.e. behave as region 2 currents [Iijima and Potemra, 1976]. In average, a dawn-to-dusk symmetry takes place in the FAC patterns. In some ranges of P_{sw} this symmetry is violated, however the deviation looks like a random spread.

FACs shown in Figure 3 should be closed to the partial ring current (PRC), flowing westward in the nightside sector. The PRC calculated as the total FAC multiplied by 2 (since the FACs flow both in the northern and southern hemispheres) is shown in Figure 4. The dependence of the PRC on P_{sw} is almost linear. The dependence on Dst is not monotonous and reveals a minimum at $Dst \approx -10$ nT. The dependence on $B_z IMF$ also exhibits a very deep minimum at

B_z IMF ≈ 0 . Similar minimums are seen in Figure 5 (left and middle), in which the dependence of P_{sw} on Dst and B_z IMF is shown. Figure 5 (right) illustrates the dependence of Dst on P_{sw} . Since the PRC depends

on both Dst and P_{sw} , and these values are statistically related, we found the three-

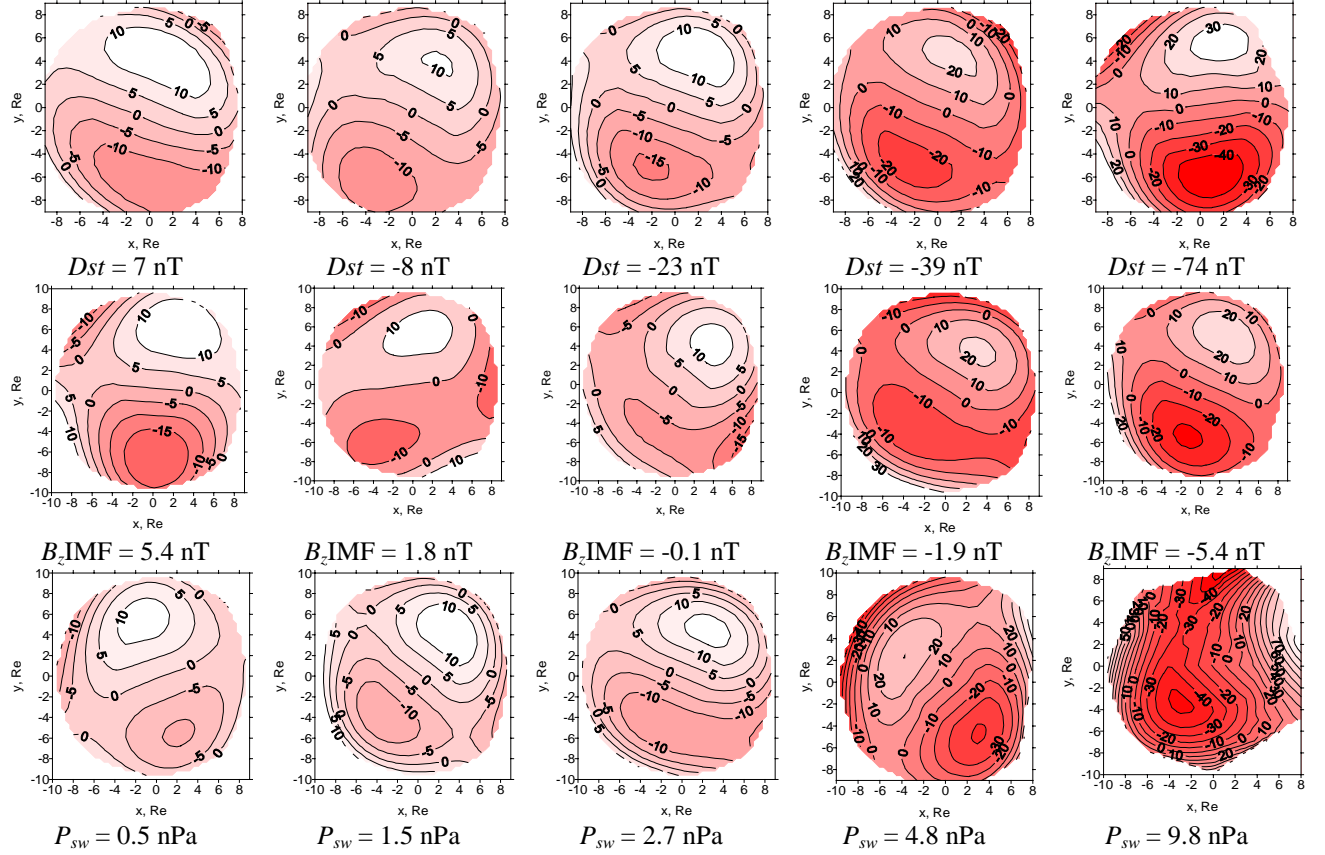


Figure 3. Field-aligned current density (in kA/R_E^2) at $z = 3 R_E$ for (top) five ranges of Dst , (middle) five ranges of B_z IMF, and (bottom) five ranges of P_{sw} .

parameter dependence $I_{PRC}(Dst, B_zIMF, P_{sw})$ by the least square technique. The following expression has been obtained

$$I_{PRC} = 0.26 + 0.55 P_{sw} - 0.15 B_sIMF - 0.023 Dst \quad (3)$$

where I_{PRC} is expressed in MA, P_{sw} in nPa, and Dst and B_sIMF in nT. The relative residual error of the fitting is 3.6%. Here B_sIMF is the IMF southward component ($B_s = 0$ for $B_z > 0$ and $B_s = B_z$ for $B_z < 0$). Fitting to B_zIMF yields a larger residual error. It is interesting that the solar wind dynamic pressure affects the PRC stronger than both the storm intensity and southward IMF. The standard deviations of P_{sw} , B_sIMF , and Dst in the 15 subsets are equal to 2.1 nPa, 1.4 nT, and 17 nT, respectively. A change of one of these parameters by the value of its standard deviation gives rise to a variation in the PRC of ~ 1.2 MA for the P_{sw} change, ~ 0.2 MA for the B_sIMF change, and ~ 0.4 MA for the Dst change.

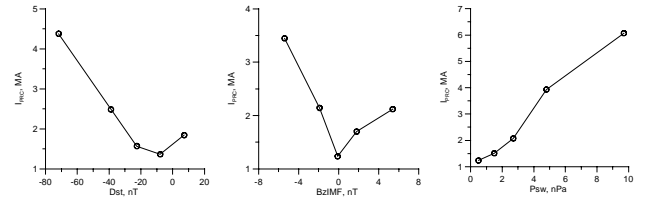


Figure 4. Partial ring current intensity versus (left) Dst , (middle) B_zIMF , and (right) P_{sw} .

The ring current near the noon can be regarded as a symmetric ring current (SRC). We obtained the following empirical relationship

$$I_{SRC} = 0.86 - 0.04 P_{sw} - 0.05 B_sIMF - 0.012 Dst$$

The relative residual error of the fitting is 78%, which is much larger than that for the partial ring current.

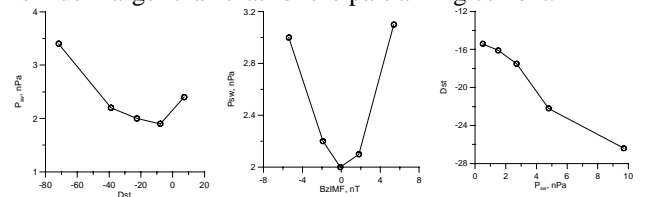


Figure 5. Dependence of (left) P_{sw} on Dst , (middle) P_{sw} on B_zIMF , and (right) Dst on P_{sw} .

5. Discussion

Our results are consistent with those by *DeMichelis et al.* [1999], who obtained the dayside ring current several times smaller than the nightside current. According to Figure 2, the noon current does not reveal any pronounced dependence on Dst , B_s IMF, and solar wind dynamic pressure. Earlier *Greenspan and Hamilton* [2000] found no essential correlation between Dst and the total plasma energy content in the dayside sector. *Turner et al.* [2001] obtained that the dayside particles contribute $\sim 75\%$ to Dst under $Dst = 0$ and $\sim 40\%$ under $Dst = -100$ nT. However, the major part of the orbit of the *Polar* satellite, which data they processed was positioned far from the equatorial plane, i.e. the satellite only detected a minor fraction of the trapped particles, namely those, which pitch-angles were sufficiently small at the equator.

Tsyganenko [1996] used the same database as we did for construction the magnetic field model T96. However, T96 practically does not reveal any day-to-night asymmetry. We emphasize that it is so because the T96 is originally based on the unrealistic assumption of the ring current symmetry. The latest model of *Tsyganenko* [2002a,b] is more accurate in this respect. We calculated the PRC intensity from this model, using the same method as was utilized in getting the curves presented in Figure 4. Instead of (3), we obtained the following approximation for the partial ring current $I_{PRC} = -0.89 + 0.68 P_{sw} - 0.05 B_s\text{IMF} - 0.026 Dst$. Thus the model slightly overestimates the role of P_{sw} and Dst and underestimates the role of $B_s\text{IMF}$.

The difference between the nightside and dayside parts of the ring current is the partial ring current (PRC), which is closed to the region 2 field-aligned currents (FACs). Since the noon ring current is small, the partial ring current is almost equal to the total nightside current. We obtained that both the PRC and region 2 FACs depend mostly on the solar wind dynamic pressure P_{sw} . *Iijima and Potemra* [1976] found the growth of the region 1/ region 2 FACs with increasing $|AL|$, the latter is known to correlate with P_{sw} (as well as with $B_s\text{IMF}$ and Dst).

6. Conclusions

Magnetic data processing in the $-3 R_E < z < 3 R_E$ range shows that the radial distribution of the ring current is not very sensitive to either the geomagnetic activity or solar wind parameters, with the current maximum being located at $6-8 R_E$. The longitudinal distribution is very asymmetric, the nightside ring current intensity being several times greater than the dayside one. The dawn-to-dusk asymmetry is rather weak. The difference between the nightside and dayside parts of the ring current presents the partial ring current presumably closed to the region 2 field-aligned currents. The partial ring current intensity is controlled mainly by the solar wind dynamic pressure. The relative effects of Dst and IMF southward component are, respectively, 3 and 6 times smaller.

Acknowledgments. This work was supported by the Russian Basic Research Foundation (grant 03-05-65379) and by the Division of Physical Sciences of the Russian Academy of Sciences (program DPS-16).

References

- Daglis, I. A., R. M. Thorne, W. Baumjohann, and S. Orsini, The terrestrial ring current: Origin, formation, and decay, *Rev. Geophys.*, 37, No 4, 407-438, 1999.
- De Michelis, P., I. A. Daglis, and G. Consolini, An average image of proton plasma pressure and of current systems in the equatorial plane derived from AMTE/CCE-CHEM measurements, *J. Geophys. Res.*, 104, No A12, 28,615-28,624, 1999.
- Dremukhina, L. A., Y. I. Feldstein, I. I. Alexeev, V. V. Kalegaev, and M. E. Greenspan, Structure of the magnetospheric magnetic field during magnetic storms, *J. Geophys. Res.*, 104, No A12, 28,351-28,360, 1999.
- Fairfield, D. H., N. A. Tsyganenko, A. V. Usmanov, and M. V. Malkov, A large magnetosphere magnetic field database, *J. Geophys. Res.*, 99, No A6, 11,319-11,326, 1994.
- Frank, L. A., On the extraterrestrial ring current during geomagnetic storms, *J. Geophys. Res.*, 72, No 15, 3753-3767, 1967.
- Greenspan, M. E., and D. C. Hamilton, A test of the Dessler-Parker-Sckopke relation during magnetic storms, *J. Geophys. Res.*, 105, No A3, 5419-5430, 2000.
- Hamilton, D. C., G. Gloeckler, F. M. Ipavich, W. Studemann, B. Wilken, and G. Kremser, Ring current development during the great geomagnetic storm of February 1986, *J. Geophys. Res.*, 93, 14,343-14,355, 1988.
- Iijima, T., and T. A. Potemra, The amplitude distribution of field-aligned currents at northern high latitudes observed by TRIAD, *J. Geophys. Res.*, 81, 2165-2174, 1976.
- Kalegaev, V. V., I. I. Alexeev, Y. I. Feldstein, L. I. Gromova, A. Grafe, and M. Greenspan, Magnetic flux in the magnetotail lobes and the dynamics of Dst disturbances during magnetic storms (in Russian), *Geomagnetism and Aeronomy*, 38 (3), 10-16, 1998.
- Korth, A., and R. H. W. Friedel, Dynamics of energetic ions and electrons between $L = 2.5$ and $L = 7$ during magnetic storms, *J. Geophys. Res.*, 102, No A7, 14,113-14,122, 1997.
- Lui, A.T.Y., and D.C. Hamilton, Radial profiles of quiet time magnetospheric parameters, *J. Geophys. Res.*, 97, No A12, 19,325-19,332, 1992.
- Lui, A. T. Y., R. W. McEntire, and S. M. Krimigis, Evolution of the ring current during two geomagnetic storms, *J. Geophys. Res.*, 92, 7459-7470, 1987.
- Smith, P. H., and R. A. Hoffman, Ring current particle distribution during the magnetic storm on December 16-18, 1971, *J. Geophys. Res.*, 78, No 22, 4731-4737, 1973.
- Spence, H. E., M. G. Kivelson, R. J. Walker, and D. J. McComas, Magnetospheric plasma pressure in the midnight meridian: Observation from 2.5 to 35 R_E , *J. Geophys. Res.*, 94, 5264-5272, 1989.
- Turner, N. E., D. N. Baker, T. I. Pulkkinen, J. L. Roeder, J. F. Fennell, and V. K. Jordanova, Energy content in the storm time ring current, *J. Geophys. Res.*, 106, No A9, 19,149-19,156, 2001.
- Tsyganenko, N. A., Effects of the solar wind conditions on the global magnetospheric configuration as deduced from data-based field models, *Proc. of the Third International Conference on Substorms (ICS-3)*, ESA SP-389, pp. 181-185, Versailles, France, 1996.
- Tsyganenko, N. A., A model of the near magnetosphere with a dawn-dusk asymmetry, 1, Mathematical structure, *J. Geophys. Res.*, 107, No A8, 10.1029/2001JA000219, 2002a.
- Tsyganenko, N. A., A model of the near magnetosphere with a dawn-dusk asymmetry, 2, Parameterization and fitting to observations, *J. Geophys. Res.*, 107, No A8, 10.1029/2001JA000220, 2002b.